ASSESSMENT OF THE APPLICABILITY OF COMPRESSION-AFTER-IMPACT (CAI) AND OPEN-HOLE TENSION (OHT) METHODS FOR USE UNDER FATIGUE LOADING

Michael R. L. Gower and Richard M. Shaw

Biomaterials, Polymers and Composites Group, Industry and Innovation Division, National Physical Laboratory, Hampton Road, Teddington, Middlesex, TW11 0LW, United Kingdom.
michael.gower@npl.co.uk

ABSTRACT

Considerable work has been undertaken to investigate the significance and assessment of defects in composite material systems, mainly resulting in the development of static test methods where specimens are loaded at a slow rate until failure. However, static loading is not totally realistic as the component is likely to experience fatigue loading rather than, or before, a static overload, and the damage is more likely to propagate to a large size, or catastrophically, under a long-term cyclic load rather than a one-off overload. This paper details a programme of experimental work designed to evaluate the applicability of static compression-after-impact (CAI) and open-hole tension (OHT) procedures for the assessment of defect criticality under constant amplitude fatigue loading. The use of an impact excitation technique for measurement of elastic properties after pre-defined numbers of load cycles and pulse thermography for detecting damage in coupons is detailed.

1.INTRODUCTION

The use of polymer matrix composite (PMC) materials can provide designers, manufacturers and end-users with a number of key advantages over traditional materials (e.g. metals, concrete etc.) including high specific strength and stiffness ratios, excellent durability, chemical and corrosion resistance, and good damage tolerance. Despite the advantages, PMC usage is still far less than their potential and that of traditional materials, which can be largely attributed to a current lack of design methodologies, reliable test methods and useable data. The situation is improving with the recent publication of a test plate manufacture standard (BS ISO 1268 [1]), a suite of harmonised ISO test methods (mechanical, thermal and physical [2]) and a data-sheet database standard (ISO 10350-2 [3]). However, there is still a requirement to develop test procedures that will allow accurate assessment of the criticality and influence of defects on the performance of composite structures, particularly under long-term loading.

The use of the static compression-after-impact (CAI) test method for laminated PMCs, where the critical loading mode (compression) is directly linked to the predominant and critical damage type (i.e. delamination) is common within the aerospace industry. Laminated wing skins are typically designed with compression performance as one of the main design drivers. Therefore compression properties need to be characterised, as they will be affected by the presence of damage within the material. The open-hole tension (OHT) test is a well-established static method for determining the effect of a hole on the tensile strength of fibre-reinforced plastic composites. The objective of this paper was to evaluate the applicability of static CAI and OHT procedures for the assessment of damage tolerance under constant amplitude and frequency fatigue loading. In addition, the use of impact excitation for measurement of elastic properties after pre-defined numbers of load cycles and pulse thermography for detecting damage in coupons is detailed.

2. EXPERIMENTAL PROGRAMME

Details of the CAI and OHT methods evaluated in this paper are now described. A unidirectional carbon fibre-reinforced epoxy system of quasi-isotropic lay-up $[+45°/0°/-45°/90°]_{2s}$ was used for both test configurations in this study. The material was supplied by Gurit Holdings AG.

2.1 Compression-after-impact (CAI) tests

The CAI test method used was ISO/CD 18352 [4]. For the impact phase, rectangular specimens (150 x 100 x ~4-5 mm) were supported on a steel base plate containing a 75 mm x 125 mm cut out. Specimens were centrally placed over the cut out region and four toggle clamps with rubber tips were used to hold the specimens flat against the test jig. The support plate was positioned centrally under the aperture of an instrumented drop weight impact tower. The energy level used was that required to cause barely visible impact damage (BVID), defined as a dent depth of 0.3 mm, which was determined by performing a series of impact tests over a range of energy levels and measuring the resulting dent depth with a laser profilometer. By plotting impact energy against dent depth, the E_{BVID} level was found by interpolation to be ~29J. Prior to performing the impact tests the force transducer on the instrumented indentor was calibrated according to a method previously developed at NPL [5]. A second strike prevention device was employed to ensure that specimens received only one impact.

For the static residual CAI tests, the CAI support jig was used on an Instron 1251 hydraulic test machine (Figure 1(a)). In order to improve the control of the test machine, the heavy base of the CAI support jig was inverted and bolted onto the load cell, which in turn was mounted on the stationary crosshead of the machine. The top loading plate was positioned on a compression platen screwed into the actuator. Alignment checks were made using two impacted, strain gauged specimens (Figure 1(b)) by monitoring the degree of bending during loading. The alignment tests resulted in less than 10% bending as per the criterion in [4]. Five static CAI tests were then undertaken at 0.5 mm/min to determine the ultimate CAI stress for use in calculating the fatigue stress levels. Unlike glass fibre-reinforced systems, the material properties of carbon fibre-reinforced plastics (CFRP) tend to be relatively insensitive to the testing rate, but in order to verify that this was the case specimens were also loaded at a rate equivalent to the fatigue rate. As expected, little difference between the strength values was observed for both the quasi-static and fatigue rate tests.

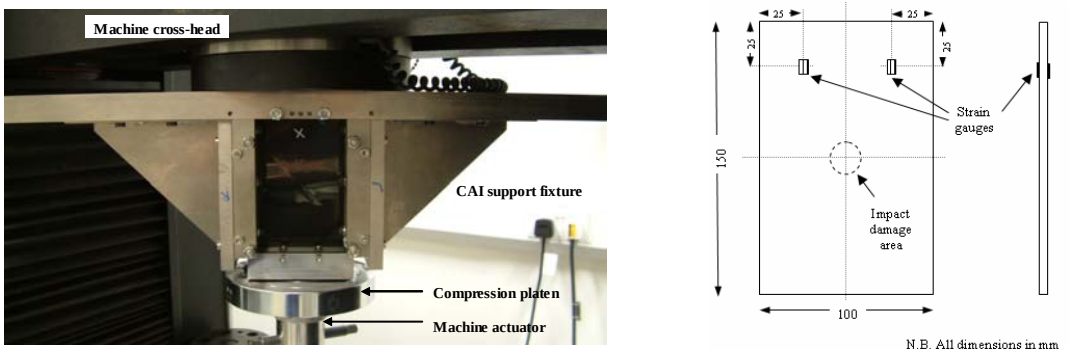

(a) (b)

Figure 1: (a) CAI fatigue test set-up and (b) strain gauge positions

For guidance on undertaking the fatigue tests, BS ISO 13003 [6] was followed. The fatigue regime used for all tests was compression-compression (stress ratio R=10). Values of σ_{min} (maximum compressive stress) were calculated as various percentages (62.5 to 85%) of the measured mean static CAI strength. Initially, it was planned to undertake 5 tests at each of 5 percentage levels of σ_{min} (as recommended in [6]), however this was varied to enable tests to be undertaken at additional stress levels so that a greater extent of the stress (S) versus number of fatigue cycles (N) plot could be investigated. Specimens were tested under load control using a sinusoidal cyclic waveform and at a test frequency of 5 Hz. Checks were made as to the extent of autogenous heating during loading. It was found that there was little or no rise in the temperature of specimens at 5 Hz. Measurement of displacement during the tests was performed using the actuator displacement. As the loading train for the CAI support jig is relatively short it was considered that there was a minimal amount of system compliance.

Specimens were tested until failure had occurred or $2x10^6$ cycles had been reached. Specimens that reached $2x10^6$ cycles without failure were classed as 'run-outs'. Data was logged on a logarithmic scale with a cycle interval of 5. Logging of each cycle was also triggered when a 5% change in the displacement amplitude was detected by the software to ensure that data was recorded close to failure.

As well as recording the number of cycles to failure, stiffness properties of each specimen were monitored throughout the test at each logged cycle. This was undertaken to assess whether changes in stiffness occurred due to growth of damage throughout the fatigue life, and whether if there was a change in stiffness, where in relation to the failure cycle it occurred. The hysteresis loop of each logged cycle was analysed to calculate the elastic and storage moduli, and damping factor. The method analysis is not described here, but can be found in [7].

In addition to the CAI tests, a set of end-loaded plain compression-compression (R=10) fatigue tests was undertaken on plain, undamaged specimens (according to a method detailed in [8]) for comparison to the CAI fatigue results.

2.2 Open-hole tension (OHT) tests

The static method used in this study is currently an ISO New work item [9]. The specimen geometry and dimensions are shown in Figure 2. The test specimen consists of a strip of rectangular cross-section with a 6 mm diameter plain hole centrally located. End-tabs are shown in Figure 2, but were not required.

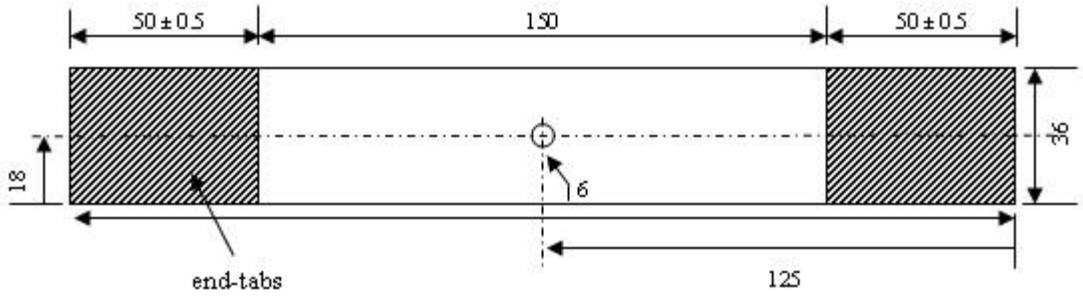

Figure 2: Open-hole tension specimen geometry and dimensions

OHT fatigue tests were undertaken using a hydraulic test machine fitted with a dynamically rated load cell. The OHT test method does not require a bespoke loading

jig as the load is introduced via mechanical wedge action grips. The grips used in this study were fatigue rated hydraulic wedge action grips and a lateral grip pressure of 200 bar was used. For the determination of the ultimate OHT stress for use in calculating the fatigue stress levels, five static OHT tests were undertaken at 1 mm/min. The maximum load sustained by the specimens was used to determine the open-hole (notched) strength based on the gross specimen cross sectional area. The static OHT method does not require the stiffness of specimens to be measured, however for the tests undertaken, efforts were made to measure the longitudinal tensile modulus and therefore detect damage accumulation, with clip gauge extensometers (50 mm gauge length).

Values of σ_{max} (maximum tensile stress) were calculated as various percentages of the measured mean static OHT strength. The maximum, mean and amplitude stress values were calculated using R=0.1. The fatigue life was to be determined by testing at least 5 specimens at each of 5 percentage levels of σ_{max}. For the OHT tests undertaken, a starting stress level of 80 % of the static OHT strength was used. However despite a large amount of damage propagation throughout the trials the result was that no failure occurred even after 10^7 cycles. Consequently, and in a deviation from BS ISO 13003, an alternative approach was adopted to investigate the effect of fatigue on specimens that exhibited extensive fatigue lives (> 10^7 cycles). Instead of running fatigue tests until failure, the approach used was to fatigue specimens at the same stress levels as would be used for the conventional approach but for pre-defined numbers of cycles. Residual strength and modulus tests were then performed on each of the fatigue specimens. Percentage stress levels of 55, 70 and 80 % of the static OHT strength were used and tests were run to 10^4, 10^5, $5x10^5$, 10^6 and 10^7 cycles.

3. DAMAGE DETECTION METHODS

3.1 Pulse thermography (PT)

Pulse thermography was used to investigate the extent of damage growth for several CAI and OHT fatigue specimens. A ThermoScope™ PT system was used for these tests. One of the key advantages of PT for damage detection compared to other techniques such as ultrasonic C-scan and X-ray, is that inspections can be performed without the need to remove specimens from the loading jig. After various numbers of fatigue cycles had been completed, tests were stopped and the specimen under test

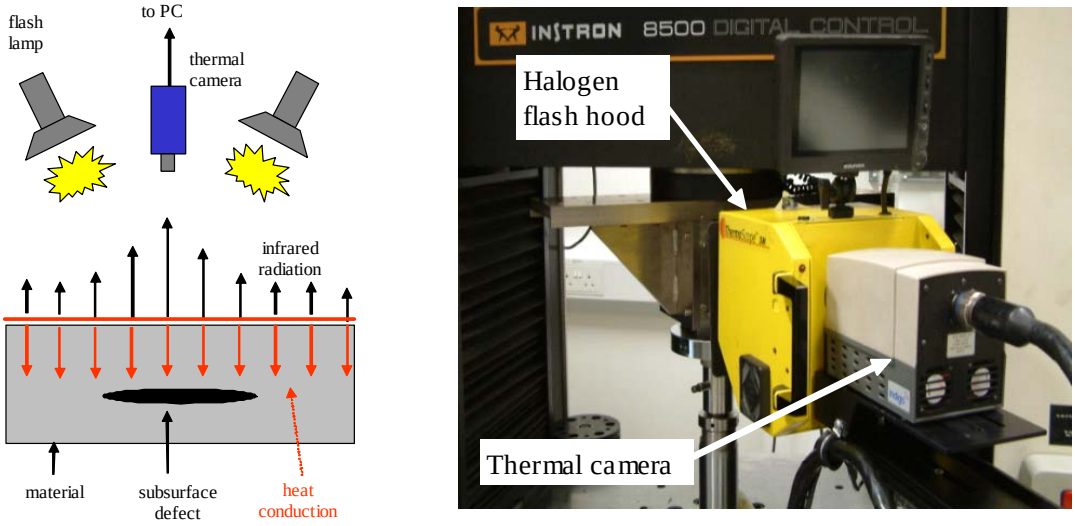

Figure 3: Principle of PT technique for damage monitoring and ThermoScope™ system adjacent to the CAI fatigue test set-up

was held briefly at the maximum compressive or tensile stress level (for CAI or OHT respectively). The specimen was then interrogated using the ThermoScope™ system before the fatigue test was resumed (Figure 3). PT can also be used to measure the depth of damage within a material, but in order to do this the system must be calibrated, ideally with the same material being inspected, or a material with a similar emissivity.

3.2 Impact excitation (IE)

Impact excitation (IE) was used to measure the elastic properties of OHT specimens by exciting various modes of vibration in general accordance with ASTM E 1876-01 [10]. (N.B. IE was not used for the CAI tests as the specimen aspect ratio was deemed unsuitable). The characteristic vibration frequencies of a beam test-piece can be determined by striking it causing 'ringing' and then deconvoluting the recorded sound spectrum. Equations can then be used to relate the resonant frequencies to elastic moduli [10]. For a prismatic beam, there are four vibration modes of interest; (i) out-of-plane flexural, (ii) in-plane flexural, (iii) torsional and (iv) longitudinal. The flexural vibration frequencies are governed primarily by the Young's modulus (E) of the test panel in the longitudinal direction, essentially independently of any material anisotropy. The torsional vibration frequencies for an isotropic material are governed primarily by the shear modulus (G) of the test-piece. If the material is anisotropic it is best if the principal axes of the test panel are parallel to the axes of anisotropy. The vibrations are governed by a mix of shear stiffness in the principal planes of the test piece containing the longitudinal direction. The longitudinal vibration frequencies are governed primarily by the Young's modulus (E) of the test panel and the Poisson's ratio in the longitudinal direction.

The IE equipment used is shown in Figure 4. It consists of an aluminium frame across which nylon support wires are stretched. The nylon wires were moved along graduated scales in order to match up to nodal positions at which positions of minimum vibration occur. The impact mechanism was a single strike with a hard ball and this was achieved using a ceramic grinding bead (4-6 mm in diameter) glued onto the end of a plastic cable-tie. In order to detect the vibrations of the test panel after it was struck, a sensitive piezosensor was placed close to the surface of the specimen at a position corresponding to an anti-node i.e. position of maximum vibration. The positions of impact and vibration detection for the various excitation modes are shown schematically in Figure 4(b).

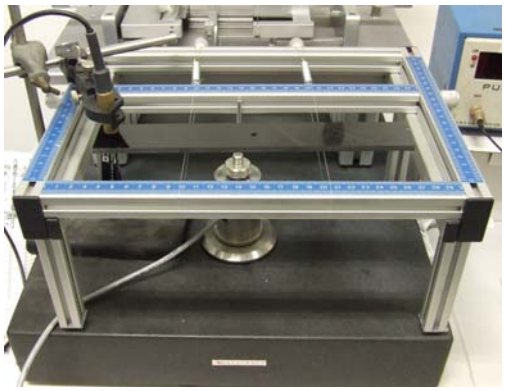

Impact mode	Schematic of impact and vibration detection locations	Elastic modulus measured
Flexural - centre strike	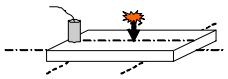	Flexural, E_f
Flexural - off-centre strike	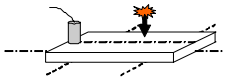	Flexural, E_f
Longitudinal end strike		Axial, E_{xx}
Flexural and torsion - end strike	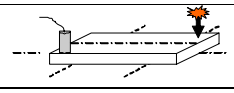	Shear, G_{xy} Flexural, E_f

(a) (b)

Figure 4: (a) IE equipment; (b) impact/vibration detection locations and moduli measured

Ideally for IE measurements, test panels should be specially prepared and have dimensions and tolerances that are specified by the relevant standard [10]. For the work detailed in this paper, specimen dimensions were dictated by the OHT test standard used. In order to identify the frequencies corresponding to the modes of vibration of interest, a modal finite element analysis (FEA) was undertaken. A comparison of measured and predicted vibration frequencies is detailed in Table 1 and shows good agreement. Values of moduli measured from the various modes of impact are also shown in Table 1 and compared to plain (un-notched) laminate data predicted using NPL Component Design & Analysis (CoDA) laminate analysis software [11]. It is noted that the presence of a hole reduces the moduli slightly in comparison to un-notched material, but in general the agreement is good. The ply properties used for the FEA and CoDA analyses were measured from mechanical tests.

Impact mode	Modulus measured	Frequency (Hz)		Modulus (GPa)	
		IE (OHT)	FEA (OHT)	IE (OHT)	CoDA (Plain)
Flexure – centre	Flexural, E_f	443	459	48.0	50.5
Longitudinal	Axial, E_{xx}	10758	11086	44.3	47.8
Flexural and torsion – end strike	Shear, G_{xy}	1662	1679	16.2	18.3

Table 1: Predicted and measured modal frequencies and moduli by impact mode

OHT specimens were fatigued to 10^4, 10^5, $5x10^5$ and 10^6 cycles at 55, 70 and 80 % of the ultimate OHT strength before being removed from the test machine and examined using the IE method. Flexural, E_f, longitudinal, E_{xx}, and shear, G_{xy}, modulus measurements were made.

4. EXPERIMENTAL RESULTS

4.1 CAI fatigue

The S-N plots for CAI and undamaged plain compression fatigue are shown in Figure 5. Figure 5(b) shows normalised compressive stress against $\log_{10}$(fatigue cycles to failure). (N.B. the scale on the vertical axis extends to 1.1 as the compressive stresses were normalised with respect to the mean ultimate compressive strength (UCS) values). In general the CAI fatigue S-N plots for both plain and CAI specimens were flat as is typically the case for CFRP materials. The plain compression S-N curve (Figure 5) exhibited a slightly steeper gradient to the CAI curve, but this was thought to be due only to the fact that fewer specimens had been tested.

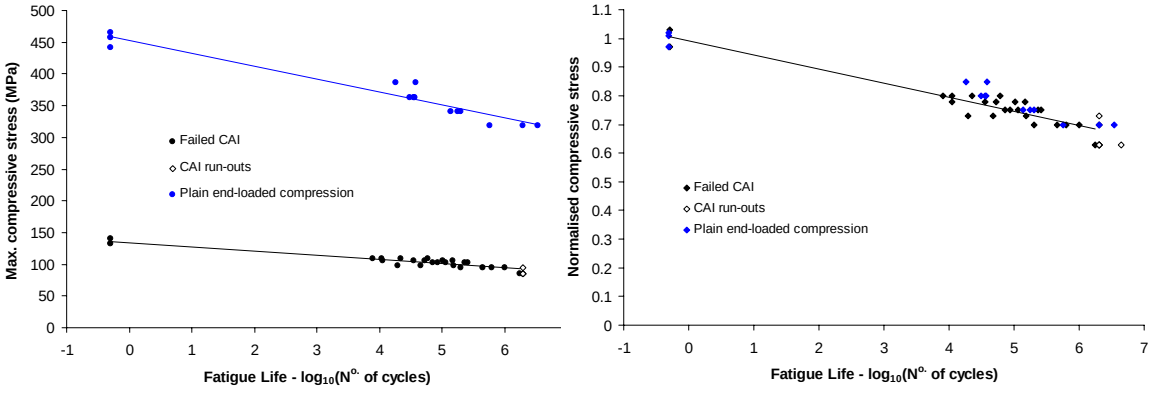

(a) (b)

Figure 5: (a) absolute and (b)normalised S-N plots for CAI and plain compression fatigue

Figure 6 shows plots of: (a) normalised elastic storage modulus against log of fatigue life, and (b) normalised storage modulus and damping factor, for tests undertaken at 80% of ultimate CAI stress. It can be seen from Figure 6(a) that the normalised compressive modulus shows minimal change over the fatigue life until close to failure. This is true for all of the percentage stress levels tested. Figure 6(b) also indicates that there are minimal changes in the storage modulus and damping factor over the fatigue life, again until just prior to failure.

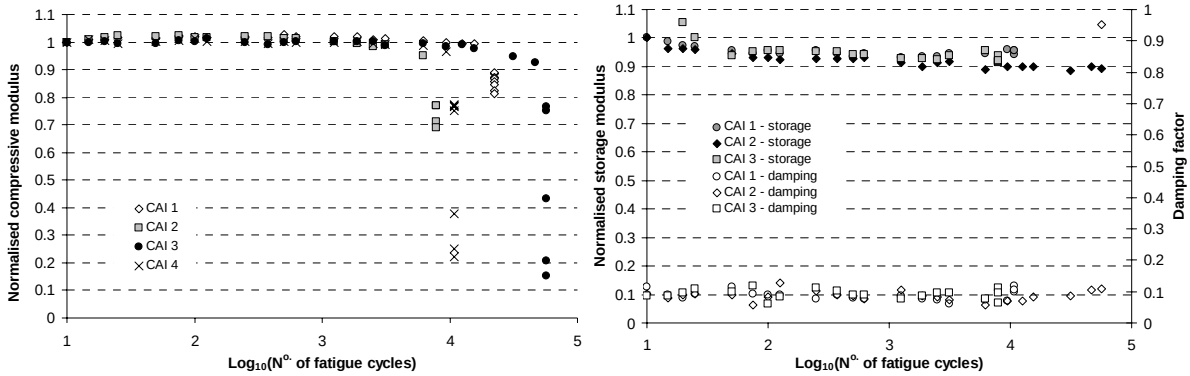

(a) (b)

Figure 6: (a) normalised compressive modulus and; (b) storage modulus and damping factor versus log of fatigue cycles for specimens tested at 80% of ultimate CAI stress

Images obtained from pulse thermographic inspection of a CAI specimen fatigue tested at 72.5 % of UCS after various numbers of fatigue cycles are shown in Figure 7. Close inspection of the damage area visible in the images indicates that there is some growth of delaminations within the specimen, but only to a minimal extent, which agrees well with the minimal changes in stiffness properties observed.

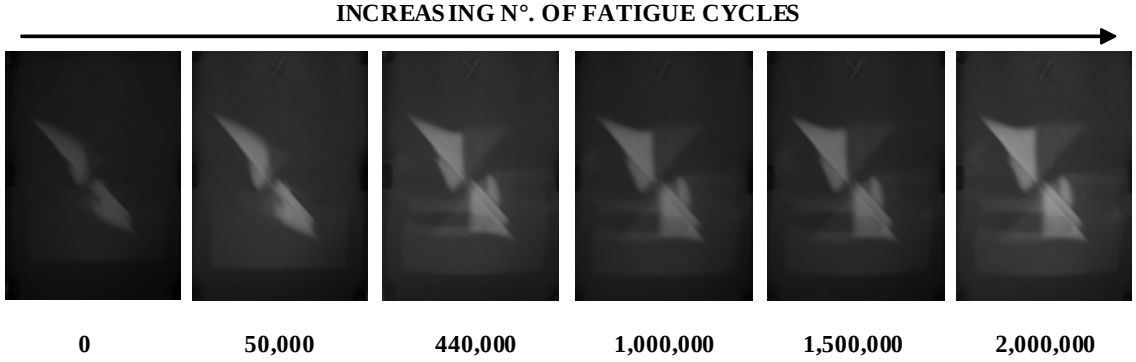

Figure 7: Pulse thermography images of CAI fatigue specimen (72.5% of static UCS)

4.2 OHT fatigue

Figure 8 shows the OHT strength and modulus plots respectively. It can be seen that the residual OHT strength tends to show initial increases with increasing fatigue cycles, until dropping away to approximately the un-fatigued OHT value or below.

The stress/strain concentration factor due to the presence of the hole lowers the tensile strength of the material. At stress levels lower than the static OHT strength, the action of fatigue causes gradual damage growth in the form of matrix micro-cracking, ply

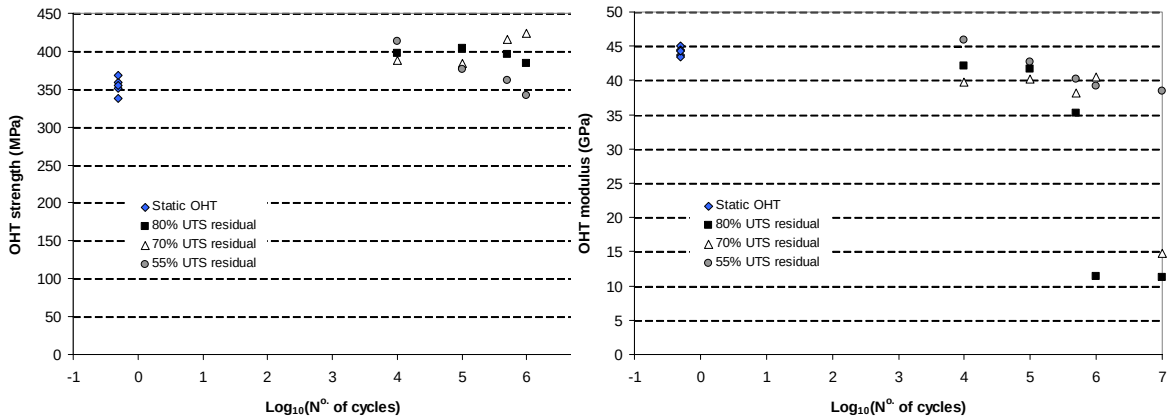

Figure 8: Residual OHT strength and modulus versus log(fatigue cycles)

splitting and delamination (the stress/strain levels are not high enough to cause fibre fracture), which in turn relieves the stress concentration around the hole. As the tensile strength of the material is dominated by the 0° plies which may contain matrix cracking, but no fibre fracture, the residual tensile strength is higher than the static OHT strength measured for undamaged specimens. After extensive fatigue, the damage reaches the extent that effectively the OHT specimen is divided into three separate parts. Damage growth is seen to propagate longitudinally along lines tangential to the hole resulting in the central portion of the specimen becoming unable to carry load. This is clearly visible in the pulse thermography image shown in Figure 9.

The trend for residual modulus values is that a decrease with increasing fatigue cycles is seen, the decrease being larger at the higher stress levels.

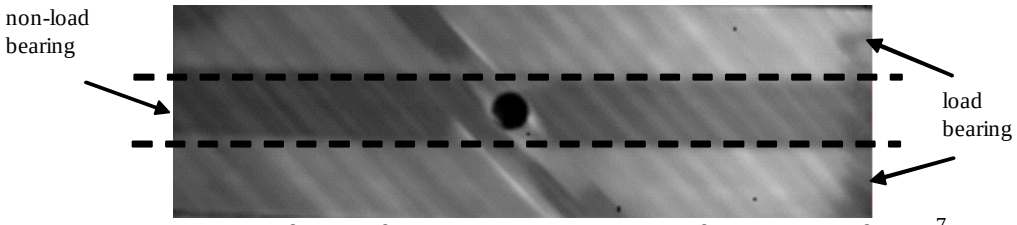

Figure 9: PT image of OHT fatigue specimen (70% of static UTS for 10^7 cycles)

Although extensometers were used throughout the fatigue tests, the extent of surface ply splitting damage resulted in the knife-edges becoming seated in ply cracks and also failure of the rubber ‘O’ rings used to attach the extensometers to the specimens. Hence, the strain data recorded was too poor for the intended hysteresis loop analysis. Strain data obtained from actuator measurements could not be used for analysis due to consequent increases in the compliance of the loading train.

The results of the flexural, longitudinal and shear modulus measurements made using the IE method are shown in Figure 10. Little or no changes in any of the moduli were seen for tests undertaken at the 55% stress level, but reductions in the shear modulus at 70% and in all moduli at 80% stress levels occur with increasing fatigue cycles. Figure 11 shows a series of thermographic images showing the degree of damage against number of fatigue cycles for the 70 and 80% OHT tests, together with the moduli values measured using IE. The reductions in moduli match well with the degree of damage present. In particular the shear modulus was observed to be sensitive to the degree of damage present.

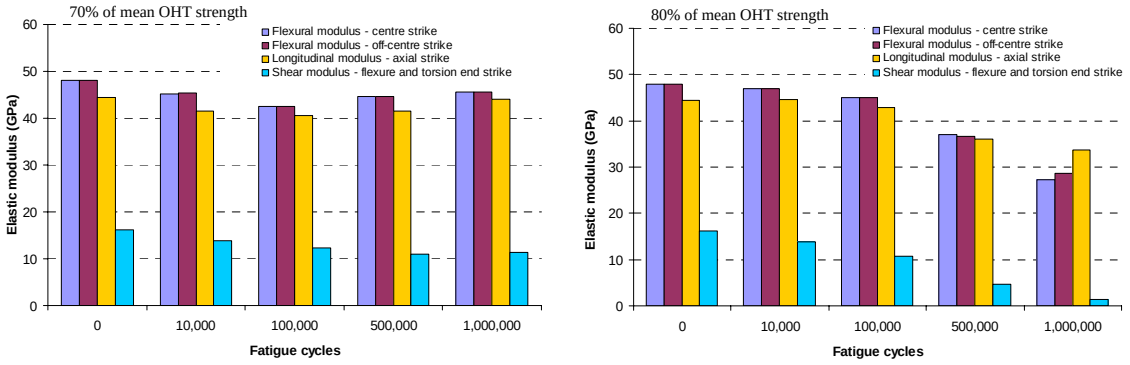

Figure 10: Elastic moduli by IE for 70 and 80% of mean static OHT fatigue specimens

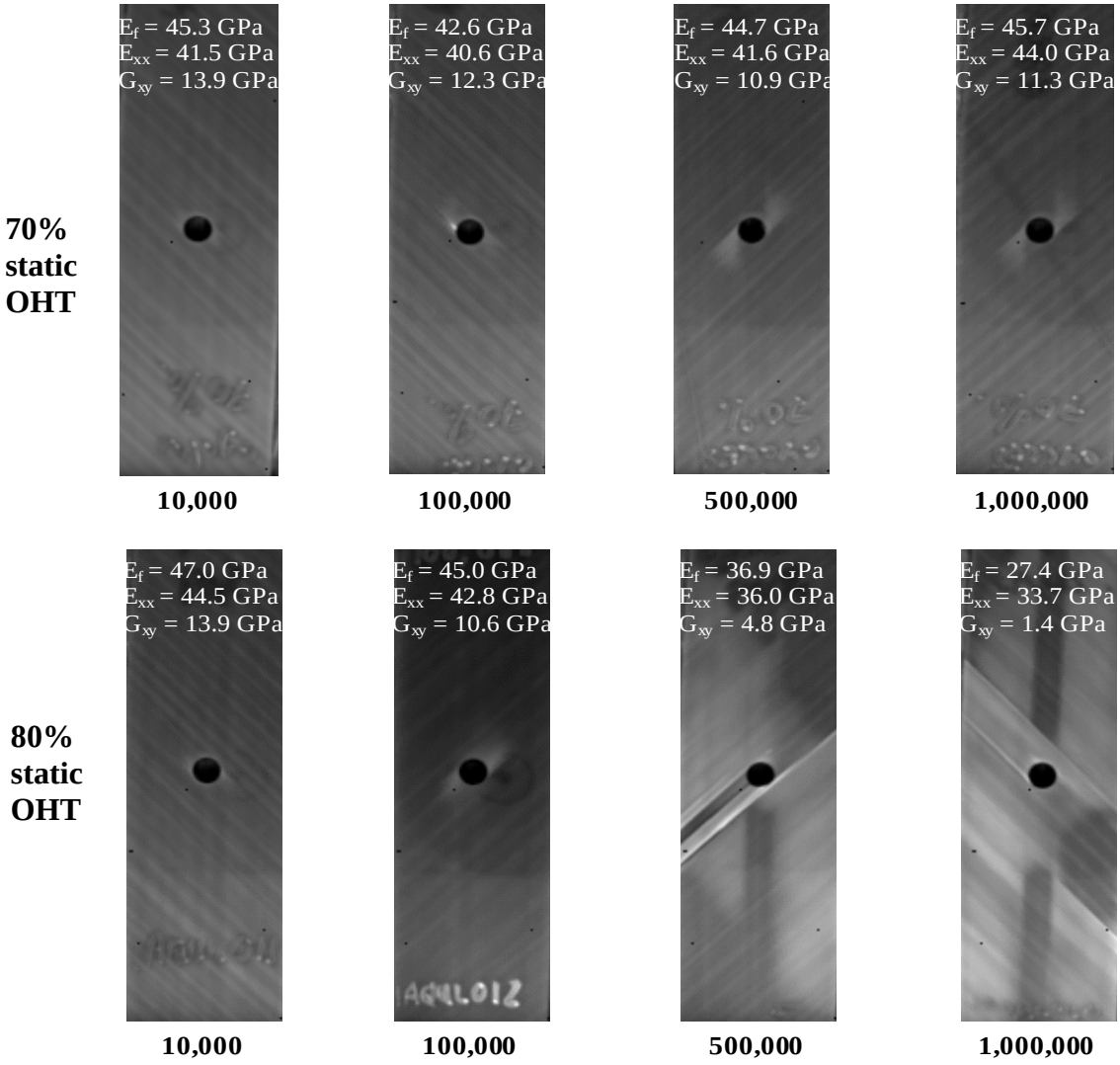

Figure 11: PT images of OHT fatigue specimens for 70 and 80% of mean static strength (moduli values measured using impact excitation)

5. CONCLUSIONS

The results of this study have evaluated the suitability and practicality of adapting static CAI and OHT test methods for use under fatigue loading. A number of key observations and conclusions are drawn. Both static methods require minimal adaptation for use under fatigue loading. The plain compression and CAI S-N curves were of similar gradient. It is reasoned that it is possible to calculate the CAI fatigue life from a 'knock-down' factor applied to the plain compression fatigue performance and knowledge of the static ultimate CAI strength. Failure of CAI fatigue specimens tended to occur suddenly with little or no reductions in compressive and storage moduli or increase in damping factor. Impact excitation has been used with some success as a relatively quick and easy method for measuring changes in elastic properties in OHT specimens, negating the requirement to perform separate mechanical tests. Pulse thermography has also been successfully used as a technique for 'on-line' damage monitoring, as it does not require the user to remove the specimen from the test jig.

ACKNOWLEDGEMENTS

The research reported in this paper was undertaken at NPL as part of the Performance Programme funded by the United Kingdom Department of Trade and Industry (National Measurement System Directorate). The authors would like to express their gratitude to the Industrial Advisory Group, Gurit Holdings AG, and NPL colleagues Dr. Graham Sims, Dr. Bill Broughton and Dr. Bruce Duncan.

REFERENCES

1. BS ISO 1268 Plastics - Preparation of glass fibre-reinforced, resin bonded, low-pressure laminated plates or panels for test purposes.
2. Gower, M.R.L. and Sims, G. D., "Fibre-Reinforced Plastic Composites - Qualification of Composite Materials", NPL Measurement Good Practice Guide N$^{o.}$ 64, 2003.
3. ISO 10350-2:2001 - Plastics - Acquisition and presentation of comparable single-point data - Part 2: Long fibre-reinforced plastics.
4. ISO/CD 18352 Carbon fibre reinforced plastics—Test method for compression after impact properties at a specified impact energy level
5. Money, M.W., and Sims, G.D., "Calibration of Quartz Load Cells; An In-Situ Procedure for Instrumented Falling Weight Impact Machines.", Polymer Testing 8, 1989, 429-442.
6. BS ISO 13003:2003 - Fibre-reinforced plastics - Determination of fatigue properties under cyclic loading conditions.
7. Gower, M.R.L., Shaw, R. M. and Sims, G. D., "Test Methods for Assessment of Damage Tolerance Under Long-Term Loading", NPL Measurement Good Practice Guide N$^{o.}$ 101, 2007.
8. BS EN ISO 14126 Fibre-reinforced plastic composites - Determination of compressive properties in the in-plane direction.
9. ISO New work item 712 - UK lead - Fibre-reinforced plastic composites - Determination of the open-hole (notched), and filled-hole, tensile strength.
10. ASTM E 1876-01 - Standard Test Method for Dynamic Young's Modulus, Shear Modulus and Poisson's Ratio by Impulse Excitation of Vibration
11. NPL CoDA PC software (Material Synthesis and Preliminary Design)